Pressure-Induced Site-Selective Disordering of $Ge_2Sb_2Te_5$: A New Insight into Phase-Change Optical Recording

A. V. Kolobov,[1,2] J. Haines,[2] A. Pradel,[2] M. Ribes,[2] P. Fons,[1] J. Tominaga,[1] Y. Katayama,[3] T. Hammouda,[4] and T. Uruga[5]

[1]*Center for Applied Near-Field Optics Research (CanFor), National Institute of Advanced Industrial Science and Technology, 1-1-1 Higashi, Tsukuba 305-8562, Japan*

[2]*Laboratoire de Physicochimie de la Matière Condensée, UMR CNRS 5617, Université Montpellier II, Place Eugène Bataillon, 34095 Montpellier Cedex 5, France*

[3]*Synchrotron Radiation Research Center, Japan Atomic Energy Agency, Kouto, 1-1-1, Sayo, Hyogo 679-5148, Japan*

[4]*Laboratoire Magmas et Volcans, Université Blaise Pascal–CNRS–OPGC, 5 rue Kessler, 63038 Clermont-Ferrand Cedex, France*

[5]*JASRI, SPring8, Mikazuki, Hyogo 679-5198, Japan*

(Received 9 February 2006; published 20 July 2006)

We demonstrate that $Ge_2Sb_2Te_5$, the material of choice in phase-change optical recording (such as DVD-RAM), can be rendered amorphous by the application of hydrostatic pressure. It is argued that this structural change is due to a very strong second-nearest-neighbor Te-Te interaction that determines the long-range order in the metastable cubic phase of $Ge_2Sb_2Te_5$ and also to the presence of vacancies. This newly discovered phenomenon suggests that pressure is an important factor for the formation of the amorphous phase which opens new insight into the mechanism of phase-change optical recording.

DOI: 10.1103/PhysRevLett.97.035701 PACS numbers: 64.70.Kb, 61.10.Ht, 61.10.Nz, 64.60.Cn

Photoinduced phase transitions are attracting ongoing attention because of their application in storage devices. The properties needed for commercial memory applications, such as fast switching, long-term stability of the photoconverted state, and high level cyclability, have singled out phase-change telluride alloys [1]. The phenomenology of phase-change optical storage is simple: Intense laser pulses melt the recording media that subsequently is quenched into amorphous bits against a crystalline background. Differences in reflectivity between the crystalline and amorphous phases serve to encode information. Although devices such as rewritable digital versatile disks (DVD-RWs) have been commercially available for over a decade, it has been only very recently that the atomic-scale mechanism of the structural changes behind the utilized transition has started to emerge [2–4].

The most used materials for commercial disks include $Ge_2Sb_2Te_5$ (GST) for DVD-RAM and Ag-In-Sb-Te alloys for DVD-RW. Interestingly, the same materials give rise to the best performance of the so-called super-resolution near-field structure (Super-RENS) disks that allow the reading of bits beyond the diffraction limit, although the readout mechanism is believed to be different from conventional phase-change memory [5]. Furthermore, the same materials are used in ovonic unified memory (OUM) [6]. It has even been argued [7,8] that phase-change memory is likely to replace the presently widespread flash memory due to its scalability and potentially unlimited rewrite capabilities. The great importance of phase-change chalcogenide alloys for advanced memory applications clearly requires a much deeper understanding of the underlying materials properties than currently exists [9].

Since pressure is an important thermodynamical parameter, it can be surmised to have a strong effect on phase stability. However, up to now, only the role of temperature has been considered in the phase diagram, which is rather unusual in the framework of thermodynamic descriptions. In this Letter, we report on the results of pressure-induced structural changes in GST.

We emphasize that pressures momentarily generated in recorded molten bits can be very large. Indeed, during melting, materials expand. Using the literature data (at 300 °C) for the thermal expansion coefficient $\partial V/V\partial T = 6.24 \times 10^5\ \mathrm{K}^{-1}$ [10], a volume increase of up to 4% is expected as GST is heated from room temperature to just above the melting point (615 °C [11]). Additionally, the density of the liquid phase (there are no data available in the literature on the density of the liquid state, and we assume it is similar to the amorphous phase) is about 7% lower than that of the metastable cubic phase [12]. A total volume expansion of over 10% is thus expected for the (freestanding) molten region. The presence of solid GST around the molten bit as well as the existence of capping layers confine the molten region that finds itself under a compressive force. Using the Hookes law and the compressibility of GeTe which is an end point of the GeTe-Sb_2Te_3 tie line [13], this force can be estimated to generate huge pressures about 5–6 GPa.

Samples were prepared by the rf sputtering of a $Ge_2Sb_2Te_5$ target [3] and were subsequently annealed at 180 °C for 2 hours in an Ar atmosphere to induce crystallization. For x-ray diffraction measurements ($\lambda = 0.71073$ Å), the annealed film was scraped off the substrate and mixed with NaCl that acted as a pressure marker; a 4:1 methanol:ethanol mixture was used as a pressure transmitting medium. Angle-dispersive x-ray diffraction (XRD) data at high pressures were measured using a diamond anvil cell. More details can be found elsewhere [14]. X-ray-absorption fine structure spectroscopy measurements were performed at SPring8 in transmission mode.

The stable GST structure is trigonal [15]. At the same time, XRD experiments on thin layers have indicated that they crystallize into a higher-symmetry metastable structure that is similar to the rocksalt structure with Te atoms forming one face-centered cubic (fcc) sublattice and Ge and Sb species occupying sites on the other fcc sublattice with 20% of the sites in the latter vacant [16]. In this work, we deal with the metastable crystal (cubic) structure that is relevant to phase-change memories. While the local structure of metastable $Ge_2Sb_2Te_5$ is distorted with Ge and Sb atoms displaced from the center of the cell [3,4,17], long-range order is best described as having the rocksalt structure with a large thermal factor, and in what follows we use pseudocubic peak indexing.

Figure 1(a) shows the pressure-induced evolution of the observed XRD pattern. One can see that, in the pressure range 0–10 GPa, compression results in a simple shift of all peaks to larger angles, indicating a decrease in the unit cell under compression. The bulk moduli K_0 and K' obtained by fitting the Birch-Murnaghan equation of state (EOS) [18] to the experimental data [Fig. 1(b)] are $K_0 = 41 \pm 2$ GPa and $K' = 3.8 \pm 0.6$. It may be informative to compare this value with the corresponding values for GeTe $K_0 = 49.9$ GPa ($K' = 3.76$) [13,19].

At higher pressures, the intensity of the GST peaks decreases and the peaks broaden: a behavior indicative of gradual amorphization. At pressures above 20 GPa, the sharp crystalline peaks are essentially replaced by a broad band that is rather similar to XRD of (as-deposited) amorphous GST [20], although a small remnant of the crystalline 220 peak is still visible. The observed amorphization is rather atypical. It can, for example, be noted that GeTe does not amorphize upon compression. Although pressure-induced amorphization has been reported for numerous materials [21], it typically happens in corner-linked polyhedral compounds, hydrogen bonded materials, and van der Waals solids. When a material with the compact rocksalt structure (both ionically and/or covalently bonded) is subject to pressure, it usually transforms to a CsCl-type structure [22,23] since the latter possesses an increased packing density.

Even more unusual is the nonuniform decrease in the relative peak intensities with increasing pressure. Figure 2 shows the pressure dependences of the normalized peak areas and full widths at half maximum (FWHM). The 111 peak disappears at pressures around 10 GPa. This is followed by the intensity decrease and subsequent disappearance of the 220 peak, while the 200 peak disappears last. The width of the 200 and 220 peaks remains constant to about 10 GPa, after which they rapidly broaden. At the same time, the NaCl 200 peak width remains constant and narrow, clearly demonstrating that the level of deviatoric stress remains low up to the maximum pressures used.

The observed pressure-induced amorphization is irreversible; i.e., the initial ''cubic'' structure is not restored upon decompression.

In what follows, we discuss a model for this rather unusual behavior of GST in comparison with the more typical case of a NaCl-type to CsCl-type transformation. Typically, in a solid the interatomic distance approximately equals the sum of the covalent (ionic) radii, and it is this distance that minimizes the bond energy. In other words, it is the first-nearest-neighbor interaction or distance that determines the lattice parameter of the crystal. Upon compression, the repulsive interaction between the first-nearest neighbors in the NaCl-type structure becomes too strong, and this is the driving force for the NaCl-type to CsCl-type transformation: The system chooses to transform into a structure with a larger first-nearest-neighbor coordination number and, hence, larger first-nearest interatomic distances which decreases the repulsion. At the same time, the second-nearest distance decreases upon transformation into the CsCl-type structure, resulting in a higher packing density.

The situation in GST is different. The first-nearest-neighbor interaction (Ge-Te and Sb-Te bonds) is rather weak as evidenced by the large mean-square relative displacement (MSRD) for Ge(Sb)-Te pairs (0.02 Å^2 [3]),

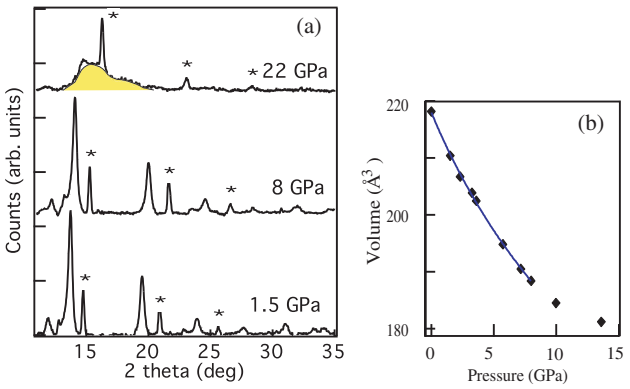

FIG. 1 (color online). (a) Pressure-induced changes of the XRD pattern of GST upon compression. The peaks marked by * are the corresponding peaks of the NaCl marker. The pressures are shown at the right side of each plot. (b) Pressure dependence of the unit-cell volume (markers) and fitting using Birch-Murnaghan EOS (solid line).

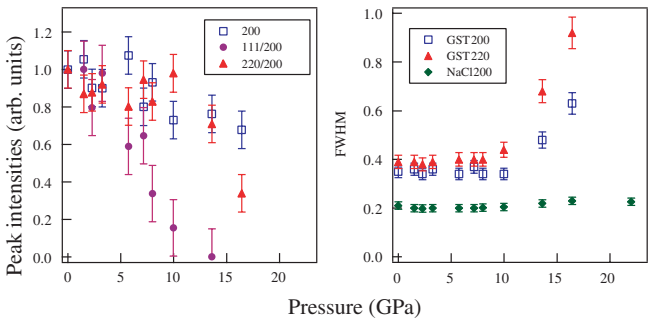

FIG. 2 (color online). Peak area (left) and peak FWHM (right) variation with pressure. The unchanged NaCl peak width indicates that hydrostatic conditions are preserved throughout the pressure range used.

which is about 4–5 times larger than in a typical covalently bonded crystal). At the same time, the second-nearest Te-Te MSRD is significantly smaller (0.01 $Å^2$ [3]) despite the longer distance, which is evidence of a very strong Te-Te interaction in GST. Based on the above, we have argued previously [3] that the long-range ordering in GST is determined by the second-nearest Te-Te interactions. For this reason, the transformation to the CsCl-like structure with the shorter second-nearest-neighbor distance is energetically unfavorable. The system seeks a way to decrease the volume without decreasing the Te-Te distance. Another important fact to be noted is that the sum of the covalent radii of Ge(Sb) and Te is smaller than half of the lattice parameter; i.e., the first-nearest-neighbor Ge-Te and Sb-Te bonds are elongated.

This ensemble of factors suggests the following scenario for the structural modification. At the initial stages of compression, the net change is a decrease in the size of the unit cell without any structural change. Up to a certain pressure, the gain in energy due to the shortening of the originally elongated Ge(Sb)-Te bonds compensates for the loss in energy due to the second-nearest-neighbor Te-Te repulsive interactions. Once the lattice parameter becomes equal to the sum of the Sb and Te radii as in the so-called hard-sphere model, Coulombic repulsion between the first-nearest Sb-Te neighbors leads to a decrease in compressibility which takes place at 10 GPa and corresponds to the lattice parameter of 5.69 Å. This value agrees very well with twice the sum of the Te and Sb covalent radii (1.40 and 1.45 Å, respectively [24]).

To get further insight into the structural modification under pressure, we have performed Ge, Sb, and Te *K*-edge extended x-ray absorption fine structure (EXAFS) measurements. The results (Fig. 3) are in perfect agreement with the above model, namely, the longer Ge(Sb)-Te bonds decrease faster than half the lattice parameter, and at pressures around 10 GPa Sb occupies a position at the center of the cell, while the shorter Ge-Te bonds remain somewhat shorter than half the lattice parameter.

Further compression leads to a drastic increase in the repulsion (now also between the first-nearest neighbors) and destabilizes the structure. At this stage, the atomic displacements are no longer isotropic due to presence of vacancies, and, as a result, the (200) planes are preferentially preserved (and their corresponding interplanar distances) until higher pressures than for the (220) planes. It is interesting to note that the suggested intermediate-range order structural changes upon laser-induced amorphization [25] also include preferential displacement of atoms along the [110] directions.

The presence of vacancies allows for significant atomic displacements; in particular, Ge atoms are likely to switch into tetrahedral symmetry positions forming four Ge-Te bonds. This atomic arrangement is more compact than the loose octahedral site. Significant atomic motion at this stage squeezes out the vacancies resulting in the required volume decrease and loss of long-range ordering. We believe that it is the rearrangement of the Ge-Te subsystem and squeezing out the vacancies that allows for the densification of the GST under pressure via transformation into the amorphous state. To check the above hypothesis, we have performed x-ray absorption near-edge structure (XANES) measurements on a sample synthesized in the multianvil apparatus after compression to 22 GPa (and subsequent decompression). XANES is sensitive to spacial arrangement of atoms, and, in particular, the spectra are quite different for Ge atoms located in octahedral (crystalline) and tetrahedral (amorphous) symmetry positions [3]. The result shown in Fig. 4 demonstrates that Ge atoms are located in tetrahedral positions as is also the case for laser-amorphized GST.

Now we address the question of why GST becomes amorphous under pressure while the binary GeTe does not. We believe that the reason is twofold. On the one hand, it may be that the presence of the second constituent (Sb_2Te_3) is needed. The different covalent radii of Ge and Sb give rise to a nonuniform strain distribution inside the material which may act as a driving force for the amorphization via nanophase separation that is often a driving force for pressure-induced amorphization [26] in cases

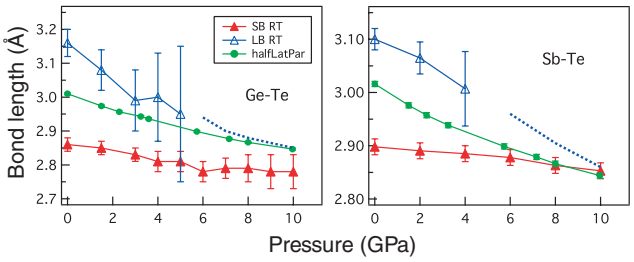

FIG. 3 (color online). Pressure-induced variations of the shorter (SB) and longer (LB) Ge-Te and Sb-Te bonds as well as the half-lattice parameter. The dotted lines show the variation of the longer bonds calculated based on the shorter bond lengths and the lattice parameter known from XRD.

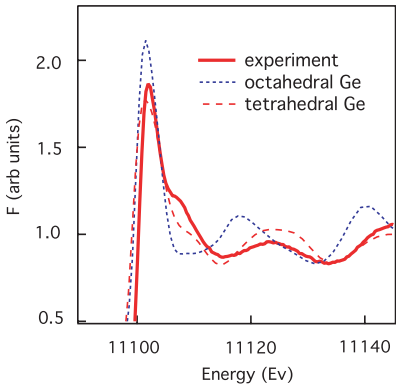

FIG. 4 (color online). XANES spectrum of GST after compression at 22 GPa and subsequent decompression. The positions of the observed features agree well with the simulated spectrum for Ge located on tetrahedral sites and are quite different from those of the octahedral "crystalline" structure.

when the total volume of the decomposed phases is smaller than the volume of the starting material. The nanophase separation into Ge-Te and Sb-Te phases was previously suggested to take place during the photoinduced amorphization [25]. At the same time, our experiments have shown that the stable trigonal phase of $Ge_2Sb_2Te_5$ (results not shown here) remains crystalline in the pressure range investigated (up to 25 GPa), which provides direct evidence of the crucial role of vacancies in the pressure-induced amorphization process.

Our results offer a new insight into the amorphous nature of the recorded bits in optical phase-change recording. As already mentioned, pressures up to 5–6 GPa are expected upon melting of a confined bit due to its expansion caused by temperature increases and amorphization. Furthermore, the surrounding area is also heated (although it remains below the melting point), leading to additional thermal expansion and thus further increasing the compressive force acting on the melt. It should also be stressed that nonhydrostatic conditions (such as shear deformation that are necessarily present in multilayered structures such as optical disks) can significantly decrease the pressure at which a phase change occurs. Thus, for GeTe, the end point of the GeTe-Sb_2Te_3 tie line, shear deformation reduces the transformation to the GeS phase by 10 GPa [19]. This factor, acting on the recorded bit just after its solidification, may further favor the creation of the amorphous phase. Finally, the application of pressure can—in some cases—lower the melting point of materials [21]. In particular, in Sb_2Te_3, the end point of the GeTe-Sb_2Te_3 tie line, the melting temperature has a minimum value at 5 GPa (a pressure range of 0–9 GPa was studied [27]). In such a case, one can expect the pressure necessary to induce amorphization to be lower that the values observed at room temperature. Experiments on the effect of temperature on pressure-induced amorphization and also studies on other phase-change materials are currently under way.

To conclude, we have observed that metastable cubic GST starts to amorphize at pressures above 10 GPa and becomes amorphous under hydrostatic pressure around 20 GPa at room temperature. We have further shown that pressures of a similar order of magnitude are generated when GST is molten under confined conditions such as for the case of a small bit in a capped layer of an optical disk. While the lack of information on the density of the liquid phase of GST does not allow us to conclude that the generated pressure is the major force that drives the bits into the amorphous state, the presented results clearly demonstrate that pressure is an important factor for the amorphization process in a device structure and should be considered on the way for improvement of current and development of novel optical disks and electrical phase-change memories for future uses. The above discussion is also applicable to OUM and other types of phase-change memories when (whatever the inducing stimuli) a recorded amorphous bit is confined within a crystalline medium or vice versa.

EXAFS measurements were carried out at SPring8 (Hyogo, Japan) at beam lines No. BL01B1 and No. BL14B1 as part of the long-term Proposal No. 2006A0006 and nanotech Proposal No. 2005A0561-CXa-np-Na. The multianvil apparatus of Laboratoire Magmas et Volcans is financially supported by the Centre National de la Recherche Scientifique (Instrument National de l'INSU).

[1] T. Ohta and S. R. Ovshinsky, in *Photo-induced Metastability in Amorphous Semiconductors*, edited by A. V. Kolobov (Wiley-VCH, Weinheim, 2003), p. 310.
[2] T. Matsunaga and N. Yamada, Jpn. J. Appl. Phys. **41**, 1674 (2002).
[3] A. V. Kolobov, P. Fons, and A. I. Frenkel *et al.*, Nat. Mater. **3**, 703 (2004).
[4] W. Welnic *et al.*, Nat. Mater. **5**, 56 (2006).
[5] J. Tominaga, in *Photo-induced Metastability in Amorphous Semiconductors* (Ref. [1]), p. 327.
[6] S. R. Ovshinsky, Phys. Rev. Lett. **21**, 1450 (1968).
[7] M. Wuttig, Nat. Mater. **4**, 265 (2005).
[8] M. H. R. Lankhorts, B. W. S. M. M. Ketelaars, and R. A. M. Wolters, Nat. Mater. **4**, 347 (2005).
[9] A. L. Greer and N. Mathur, Nature (London) **437**, 1246 (2005).
[10] N. Yamada and T. Matsunaga, E*PCOS2003, extended abstracts.
[11] N. K. Abrikosov and G. T. Danolova-Dobryakiva, Izv. Akad. Nauk SSSR, Neorg. Mater. **1**, 204 (1965).
[12] T. P. L. Pedersen, J. Kalb, and W. K. Njoroge *et al.*, Appl. Phys. Lett. **79**, 3597 (2001).
[13] A. Onodera, I. Sakamoto, and Y. Fujii *et al.*, Phys. Rev. B **56** 7935 (1997).
[14] J. Rouquette *et al.*, Phys. Rev. B **65**, 214102 (2002).
[15] I. I. Petrov, R. M. Imamov, and Z. G. Pinsker, Sov. Phys. Crystallogr. **13**, 339 (1968).
[16] N. Yamada and T. Matsunaga, J. Appl. Phys. **88**, 7020 (2000).
[17] S. Shamoto *et al.*, Appl. Phys. Lett. **86**, 081904 (2005).
[18] F. Birch, Phys. Rev. **71**, 809 (1947).
[19] N. R. Serebryanaya, V. D. Blank, and V. A. Ivdenko, Phys. Lett. A **197**, 63 (1995).
[20] W. K. Njoroge, H. W. Woltgens, and M. Wuttig, J. Vac. Sci. Technol. A **20**, 230 (2002).
[21] S. M. Sharma and S. K. Sikka, Prog. Mater. Sci. **40**, 1 (1996).
[22] D. Zahn and S. Leoni, Phys. Rev. Lett. **92**, 250201 (2004).
[23] P. Toledano, K. Knorr, and L. Ehm *et al.*, Phys. Rev. B **67**, 144106 (2003).
[24] http://www.webelements.org
[25] A. V. Kolobov, P. Fons, and J. Tominaga *et al.*, Jpn. J. Appl. Phys. **44**, 3345 (2005).
[26] A. K. Arora, Solid State Commun. **115**, 665 (2000).
[27] L. G. Khvorostyantsev *et al.*, Phys. Status Solidi A **89**, 301 (1985).